# CCAT: Mod-Cam Readout Overview and Flexible Stripline Performance

Ben Keller, Rodrigo Freundt, James R. Burgoyne, Scott Chapman, Steve Choi, Cody J. Duell, Christopher Groppi, Caleb Humphreys, Lawrence T. Lin, Alicia Middleton, Michael D. Niemack, Darshan Patel, Eve Vavagiakis, Samantha Walker, Yuhan Wang, Ruixuan (Matt) Xie

***Abstract*—The CCAT Observatory's first-light and commissioning instrument, Mod-Cam, is nearing readiness for deployment to the Fred Young Submillimeter Telescope (FYST) in the Atacama Desert in northern Chile. In-lab testing of Mod-Cam and the first CCAT instrument module, a 280 GHz broadband camera fielding over 10,000 kinetic inductance detectors (KIDs), is currently underway. CCAT's first-generation science instrument, Prime-Cam, will field approximately 100,000 KIDs across seven instrument modules. Like Mod-Cam, it employs 46 cm long low-thermal-conductivity flexible circuits ("stripline") between 4 K and 300 K to connect large arrays of multiplexed detectors in each instrument module to readout electronics. The 280 GHz camera currently installed in Mod-Cam uses six striplines to read out its over 10,000 detectors across 18 RF chains, each individual stripline containing six traces. In-lab testing thus far has allowed us to begin optimizing the attenuation in the readout chains for each of the three detector arrays in the 280 GHz module and demonstrate simultaneous readout of all networks using CCAT's RFSoC warm readout electronics. Here we present an overview of the Mod-Cam cold readout and discuss the stripline performance by investigating how its thermal conductivity impacts Mod-Cam and Prime-Cam cryogenic performance. We also report on stripline electrical transmission and crosstalk, identifying transition printed circuit boards (PCBs) as the dominant source of crosstalk. Using this result we outline design improvements to these PCBs that enhance isolation between readout networks.**

***Index Terms*—CMB, KID, readout, flexible circuits, instrumentation**

## I. Introduction

The CCAT Collaboration is currently constructing the Fred Young Submillimeter Telescope (FYST), a six-meter off-axis crossed-Dragone telescope, at an elevation of 5600 m on the summit of Cerro Chajnantor in the northern Chilean Atacama Desert [1]. Due to the low precipitable water vapor (PWV) at the telescope site [2], FYST will offer an unprecedented view into the sub-millimeter sky, with observations scheduled to begin in 2026. The CCAT Collaboration has been assembling and testing two instruments to be housed in FYST: the first-light testbed instrument Mod-Cam, and the first generation science instrument Prime-Cam. These instruments will make broadband polarimeteric observations at frequencies ranging between 280-850 GHz with additional spectroscopic surveys performed at 210-420 GHz with $R \sim 100$ [3], targeting science goals ranging from understanding the growth of structure during the Epoch of Reionization to constraining cosmology using measurements of the Sunyaev-Zel'dovich (SZ) effect [4].

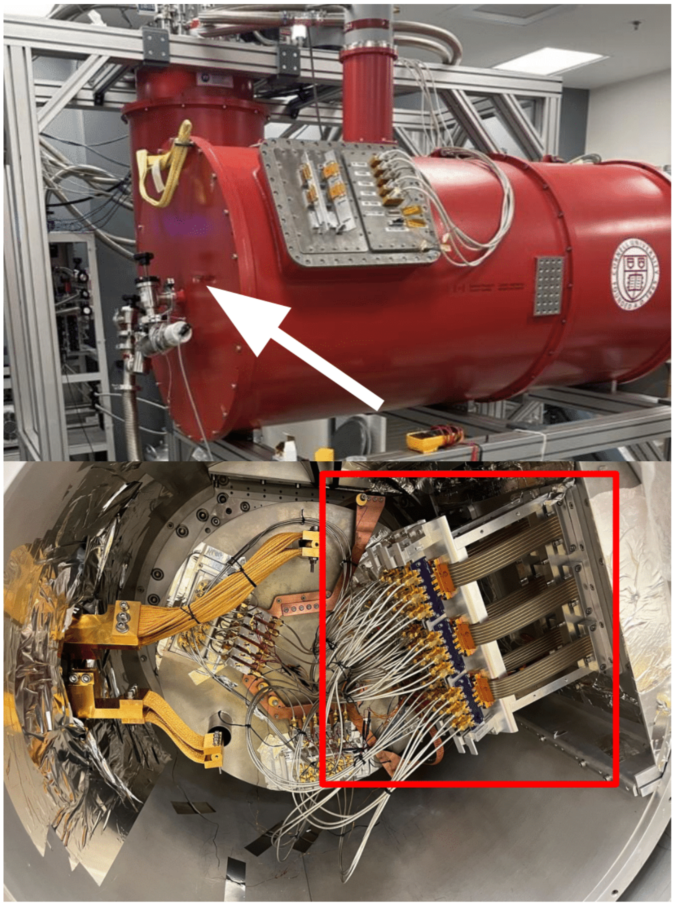

Fig. 1. Picture of Mod-Cam from the side (above) and the back of Mod-Cam when the cryostat is open after instrument module installation (below). The white arrow denotes the location of the back of Mod-Cam. When the back vacuum shells are open, the mounting scheme for the six striplines is clearly shown (boxed in red), along with the purple transition PCBs and coax interface to the 4 K low noise amplifiers mounted on the copper heatsink.

B. Keller, C. J. Duell, R. Freundt, C. Humphreys, L. T. Lin, M. D. Niemack, D. Patel, S. Walker, and Y. Wang are with the Department of Physics, Cornell University, Ithaca, NY 14853, USA. (e-mail: bdk54@cornell.edu).

J. R. Burgoyne and R. Xie are with the Department of Physics and Astronomy, University of British Columbia, Vancouver, BC V6T 1Z1, Canada

S. Chapman is with the Department of Physics and Atmospheric Science, Dalhousie University, Halifax, NS B3H 4R2, Canada.

S. Choi is with the Department of Physics and Astronomy, University of California, Riverside, CA 92521, USA.

C. Groppi is with the School of Earth and Space Exploration, Arizona State University, Tempe, AZ 85287, USA.

E. Vavagiakis is with the Department of Physics, Duke University, Durham, NC, 27704, USA, and the Department of Physics, Cornell University, Ithaca, NY 14853, USA.

Mod-Cam is a cryogenic receiver with a side-car dilution refrigerator (DR) design featuring space for a single instrument module [5]. Mod-Cam has been used extensively as an in-lab testbed for the first CCAT instrument module, a 280 GHz broadband camera. The 280 GHz module features over 10,000 KID detectors split across three arrays, each with six networks of $\sim 570$ detectors [6]. To connect the detectors to the warm RFSoC readout electronics, Mod-Cam employs six 46 cm low-thermal-conductivity flexible circuits ("stripline") between 4 K and 300 K.

Prime-Cam, CCAT's primary science instrument, has also recently been assembled for the first time at Cornell and is currently undergoing cryogenic validation. Prime-Cam features space for seven modules, all with the same mechanical form as the 280 GHz camera. Additional modules currently under construction are the 350 GHz and 850 GHz broadband cameras, as well as the EoR-Spec spectrometer module [7][3]. Additional spectrometer-on-a-chip module designs are planned.

To read out seven instrument modules with $\sim 100,000$ total KIDs, Prime-Cam has three readout ports, often colloquially referred to as readout harnesses. Current plans feature the 280 GHz, 350 GHz, and EoR-Spec modules being read out through a single readout harness with 18 striplines, utilizing 48 of the available 54 readout chains (six chains, or two full stripline being reserved as spares). The design for the first readout harness is shown in Fig. 2. This readout harness will utilize the same 46 cm flexible circuitry as is installed in Mod-Cam, although changes have been made to the circuit geometry to reduce thermal loading at the 4 K stage where the heat budget is limited. These updated designs feature half the copper pour thickness in the signal and ground traces (9 $\mu$m) along with a roughly doubled length of circuit (20 cm) between the 4-40 K stages as compared to the designs in Mod-Cam. Fabrication of the Prime-Cam stripline and first readout harness with these modifications is currently underway.

In this work we present an overview of the stripline currently installed in Mod-Cam. We characterize the thermal conductivity of the circuit by measuring both the residual resistance ratio (*RRR*) and the thermal conductivity-temperature relation for the copper traces in the flexible circuits. Using the *RRR* measurement, we also obtain thermal loading estimates for the stripline configurations in both Mod-Cam and Prime-Cam. We then present measurements of the room-temperature transmission and crosstalk through the stripline and transition printed circuit boards (PCBs) used to interface with readout coax, isolating the source of elevated crosstalk in the Mod-Cam readout chains to the transition PCBs. Improvements to the PCBs in light of this result are discussed.

## II. Mod-Cam Cryogenic Readout and Stripline Design

The 280 GHz broadband instrument module currently installed in Mod-Cam features three KID arrays read out across 18 total RF chains; these RF chains use 304 Stainless Steel coax on the inputs from 0.1-4 K and NbTi coax on the outputs from 0.1-4 K [6]. There is a mixture of attenuation installed at 0.1 K, 1 K, and 4 K on the input side of the readout chains.

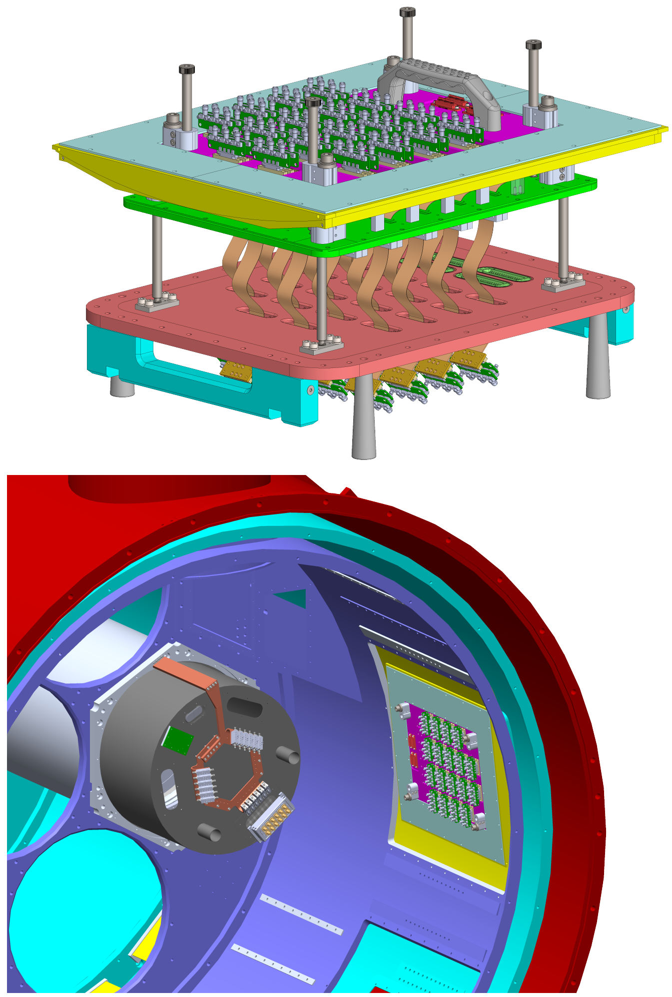

Fig. 2. Rendering of the first Prime-Cam readout harness with 18 stripline assemblies installed (above) and the full readout harness inserted into a Prime-Cam model (below). The geometry of this stripline reflects the changes discussed in Section I. The red, green, and yellow plates seen in the readout harness are mounted to the Prime-Cam 300, 40, and 4 K shells respectively. Temporary installation rods that aid in holding the readout harness together before the plates are secured to the cryostat shells are included in the model; these rods are removed after installation.

Optimization of the chain attenuation for thermal stability of the focal plane and readout noise is ongoing. Cryogenic low noise amplifiers manufactured at Arizona State University are connected to the outputs and physically mounted at 4 K on the back of the instrument module, as seen in Fig. 1. Flexible coax connects the chains to the stripline installed in Mod-Cam via an SMP-SMA transition PCB.

From 4 K to 300 K, Mod-Cam employs six stripline assemblies to bring signals into and out of the instrument module. The stripline characterized in this paper and installed in Mod-Cam utilizes 46 cm long flexible circuits manufactured by DuPont with a buried copper signal layer sandwiched between polyimide, with outer copper ground layers on either side spanning the length of the circuit [8]. At designated clamping points the ground plane is extended fully across the width of the circuit to provide better thermal contact

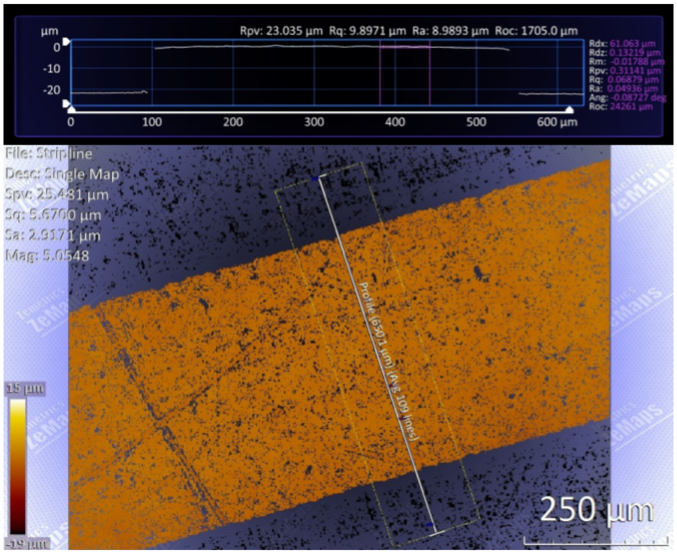


Fig. 3. Profilometry of a ground trace on a stripline assembly showing the trace thickness to be approximately 22 $\mu$m thick and 0.43 mm wide.

with heat sinking clamps at the 4 K and 40 K stages in the cryostat. The ground traces are otherwise kept to $0.43$ mm width to minimize thermal conductivity along the length of the circuit. Profilometry in Fig. 3 shows the ground traces are measured to be approx. 22 $\mu$m thick. Original designs called for trace dimensions of $18\mu m$ thickness and $0.38$ mm width. The additional cross-sectional area is believed to result from the gold plating being thicker than expected.

The complete stripline assemblies are built at Arizona State University, where each end of the circuit is soldered to two custom Delta RF 3-port SMP connectors. The circuit is then epoxied into a vacuum flange at a fixed location. On the back of each connectorized region, a thin G10 tab is added for mechanical rigidity and and to protect the circuit when SMP connections are made and unmade. The stripline interface with coax at 4 K and 300 K uses a custom transition PCB designed at Cornell that takes the 3-port SMP connectors and converts them to SMA connections. A stripline assembly and an accompanying transition PCB are shown in detail in Fig. 6.

## III. Thermal Characterization of Stripline

### A. *RRR Measurement*

To measure the Residual Resistance Ratio (*RRR*) value of the copper in the flexible circuit, we cut a section of stripline approximately 5 cm long and mounted it to a PCB for installation on the 4 K stage of a Bluefors LD400 dilution refrigerator. Using a Lakeshore 372 AC resistance bridge, we measured the resistance of the copper trace at 300 K and 4 K, taking the ratio as the *RRR* value. The length of the measured trace was chosen to ensure that the smaller 4 K resistance would remain well within a viable range for accurate measurement with the Lakeshore 372.

The 300 K resistance of the segment of copper trace was measured at $275\ \mathrm{m}\Omega$, while the 4 K resistance was measured at approximately $2.3\ \mathrm{m}\Omega$. We assume that the Au plating on the copper trace negligibly contributes to the overall trace

TABLE I
Thermal loading estimates through the stripline between two sets of temperature stages: 300 K to 40 K, and 40 K to 4 K.

| | Mod-Cam Stripline Loading (W) | Prime-Cam Stripline Loading (W) |
|---|---|---|
| Per Network (300 K to 40 K) | $2.0 * 10^{-2}$ | $7.3 * 10^{-3}$ |
| Per Stripline (300 K to 40 K) | $1.2 * 10^{-1}$ | $4.4 * 10^{-2}$ |
| **Per Readout Harness (300 K to 40 K)** | **0.71** | **0.79** |
| Per Network (40 K to 4 K) | $1.8 * 10^{-2}$ | $4.9 * 10^{-3}$ |
| Per Stripline (40 K to 4 K) | $1.1 * 10^{-1}$ | $3.0 * 10^{-2}$ |
| **Per Readout Harness (40 K to 4 K)** | **0.64** | **0.53** |

resistance. The resulting ratio of resistances yields a *RRR* $\approx$ 120. This value is consistent with high-purity OFHC copper and supports the use of the cryogenic thermal conductivity functional form $k(T)$ from literature [9].

Using the measured *RRR* value for these circuits and the functional form of cryogenic OFHC copper thermal conductivity given by Simon et al. [9], we obtain estimates for the thermal loading in Mod-Cam and Prime-Cam from the 300-40 K and 40-4 K stages for the configurations described in Section I. The estimates are obtained using the equation for linear thermal conductivity:

$$k = \frac{Pd}{A\Delta T}, \quad (1)$$

where $k$ is the thermal conductivity of the material, $P$ is the transmitted power between two ends of the material, $d$ is the distance between the ends, $A$ is the cross-sectional area of the material, and $\Delta T$ is the temperature difference between the two ends.

For Mod-Cam, $\Delta T$ is given by real measurements of the Mod-Cam temperature stages, where the temperature of the 4 K readout mount is consistently about 12 K while the 40 K readout mount is consistently about 51 K. Based on thermal budgets and loading estimates for Prime-Cam, we anticipate a realistic temperature of the 4 K readout harness will be 4 K, while the 40 K harness will be no warmer than 53 K. The thermal conductivity used in these estimates $k$ assumes a linear gradient between two temperatures and is obtained by numerically integrating the functional form of $k(T)$ between the two temperatures to obtain $k_{avg}$ in the given range. For Mod-Cam estimates, $A$ is given by the profilometry measurements shown in Section II and $d = 0.115$ m is set by the physical design of the stripline. For Prime-Cam estimates the physical dimensions used reflect the changes outlined in Section I. The estimates obtained for the thermal loading from stripline in both Mod-Cam and Prime-Cam are compiled in Table I.

### B. *Thermal Conductivity Measurement*

Thermal conductivity measurements were performed in a Bluefors SD250 Dilution Refrigerator with a custom mount allowing the stripline to be suspended from the 4 K stage. The mounting scheme is described in detail in Fig. 4. To perform the measurement, we applied a current to the hot-side heater while measuring the temperatures of the hot and cold sides of the stripline, $T_h$ and $T_c$ respectively, with Cernox 1050-CD

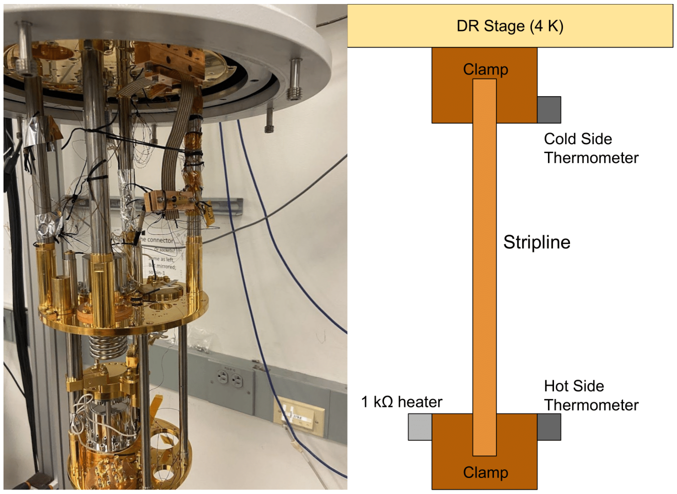


Fig. 4. A photograph of the testing setup used for 4 K thermal loading measurements is shown (left) along with a schematic diagram of the testing setup (right). Hot and cold side temperatures, $T_h$ and $T_c$ respectively, are each measured using a Cernox cryogenic temperature sensor. Thermal loads are applied across the stripline with a 1 kΩ resistor sunk to the warm side clamp.

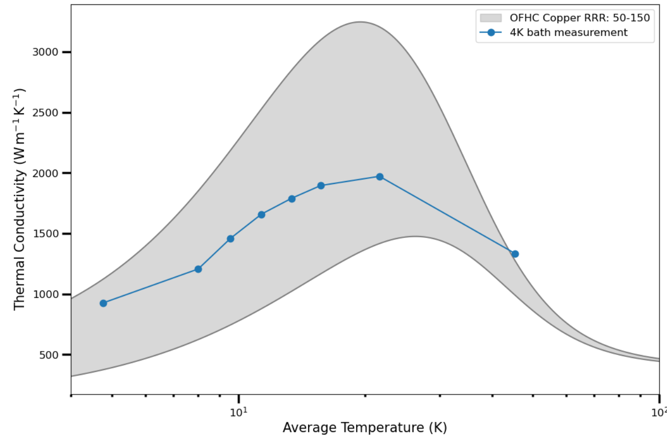


Fig. 5. The measured thermal conductivity of the stripline is plotted against the average temperature of the hot and cold sides of the circuit with gray overlay denoting the functional form of OFHC copper thermal conductivity from [9] for $RRR = 50$ on the lower bound to $RRR = 150$ on the upper bound.

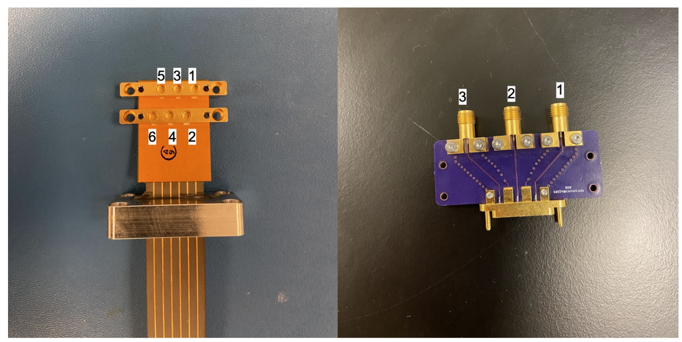


Fig. 6. Left: The connectorized end of one stripline circuit. The numbers denote the labeling scheme used in Fig. 7 top and middle panels. Right: Photograph of the SMP-SMA transition PCB. Two PCBs plug into each end of the stripline. The numbers denote the labeling scheme used in the bottom panel of Fig. 7.

thermometers. This process was repeated for various currents, and thus heater powers, while the stripline was heat sunk at 4 K on the cold side. Heater powers were ramped to achieve temperature gradients comparable to those measured in Mod-Cam.

During testing, thermometers and heaters were equipped with long manganin cables to ensure the primary path for heating was through the stripline itself. Additionally, heater resistances were chosen to ensure that dissipated heat primarily occurred in the resistor, as opposed to the long wires extending from it. Estimates of radiative power transfer to the stripline in the range of measured hot-side clamp temperatures are negligible compared to the powers applied through the heater.

Using Eq. 1 and the temperature gradient measured across the stripline for each applied power, the thermal conductivity as a function of average temperature of the hot and cold sides of the stripline is found. Geometric factors used in Eq. 1 are given by profilometry measurements in Section II and measurements of the distance between clamps. At cryogenic temperatures, the thermal conductivity of polyimide is known to be more than 4000x smaller than that of copper [10], so thermal conduction through the polyimide dielectric is assumed to be negligible compared to the circuit copper layers. The result of the measurement is shown in Fig 5. The direct measurements of thermal conductivity agree with calculated values using similar $RRR$ values to those reported in Section III-A.

## IV. Crosstalk

### A. Measurement

During in-lab testing of the 280 GHz instrument module we observed elevated crosstalk through the full readout chain. Cold measurements confirmed no significant reflections in the readout chains, so we are confident excess pickup is primarily occurring between different readout chains. We sometimes refer to this as inter-channel crosstalk. In order to isolate the source of this crosstalk, we perform warm S21 measurements using an Agilent E5071C VNA over the full readout bandwidth for the TiN and Al arrays installed in the 280 GHz module, which combined span a range from 300 MHz - 1.5 GHz. Crosstalk measurements are performed for a variety of configurations: a lone stripline, a stripline with a SMP-SMA transition PCB connected on either end (mimicking the readout structure in Mod-Cam), and a lone transition PCB.

### B. Crosstalk Measurement Results

Warm S21 measurements of the various configurations are shown in Fig. 7, with labels corresponding to connections designated in the labeling scheme in Fig. 6. The results demonstrate that the stripline alone is not the dominant source of crosstalk in the readout chain, with inter-channel crosstalk 50 dB or more below transmission, meeting project requirements. The middle panel of Fig. 7 isolates the source of crosstalk in the readout chain to the custom transition PCBs; in this configuration, chains 2, 4, and 6 share the same PCB and show elevated crosstalk, up to 30 dB above those

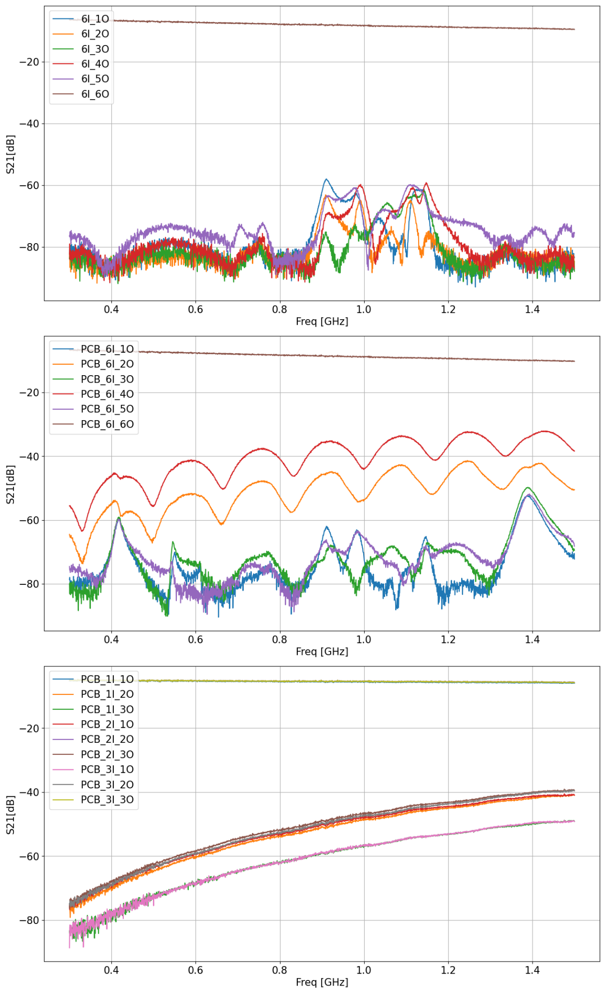


Fig. 7. Warm crosstalk measurements are shown. The top panel shows the crosstalk measured for all channel combinations with a single channel (6) in an isolated stripline. The labeling scheme indicates the Input (I) and Output (O) with each associated channel number. Transmission through channel 6 is observed at the top of the plot. The middle panel shows crosstalk measured through the combination of a stripline with a SMP-SMA transition PCB on either end. The bottom panel shows crosstalk measured through an isolated transition PCB.

combinations that do not share a PCB. The level of crosstalk is also correlated with physical spacing on the transition PCB, with closer traces observing higher pickup; this accounts for the elevated level of the "6I_4O" measurement relative to the "6I_2O" measurement.

In light of this result, the SMP-SMA transition PCBs have been redesigned using an impedance matched via to quickly bury the signal trace in an intermediate PCB layer between ground planes for improved isolation. Given the frequencies of the readout band, radiative effects from the via ends are expected to be minimal. Moreover, our ability to isolate signal traces on the PCB is fundamentally limited by the ganged SMP connector design, which is necessarily mounted on the edge of the PCB board. At minimum, this results in a small section of microstrip trace on the PCB which can add crosstalk. The original PCB design referenced in Fig. 6 and Fig. 7 utilized only microstrip traces.

To estimate the predicted crosstalk of this new design we performed simulations of the microstrip-to-stripline transition via structure using Ansys HFSS software. Using these simulations we first optimize the microstrip, stripline, and via dimensions to impedance match the full structure to 50 $\Omega$. Using a simulated PCB configuration with optimal trace and via dimensions, the simulations yield crosstalk estimates at a level no greater than -60 dB for a single structure, and -57 dB across the full PCB. This represents an approximately 20 dB improvement in crosstalk level over the old PCB design, which should allow the PCB to exceed project requirements.

## V. Conclusion

We performed two types of measurements to characterize the thermal loading through the stripline flexible circuitry designed for Mod-Cam and Prime-Cam: finding the $RRR$ of the copper traces and directly estimating the thermal conductivity of the circuit as a function of temperature. The measured thermal conductivity values are consistent with theoretical values common in literature. With the materials of the stripline characterized, we then predicted the expected thermal loading for nominal stripline configurations for both Mod-Cam and Prime-Cam. Results of these predictions demonstrate the significant improvement in expected loading levels for the redesigned Prime-Cam stripline; despite being populated with three times more stripline, the estimated loading at 4 K through one Prime-Cam readout harness is actually lower than the Mod-Cam readout harness.

When in-lab testing of the readout in Mod-Cam yielded higher-than-anticipated crosstalk through the readout chains, we performed measurements to isolate the source of this pickup. Results of this testing identified the source to be the SMP-SMA transition PCBs, which carry signals from the stripline flexible circuits into coax cables. Subsequent redesign and simulation of these PCBs has demonstrated that they should meet project requirements for low crosstalk when fabricated.

Flexible stripline circuits installed in Mod-Cam have proven to be a robust option for the simultaneous readout of thousands of KIDs during months of in-lab testing. The results presented in this paper validate stripline as a scalable solution for readout of large KID arrays and inform the ongoing fabrication of optimized Prime-Cam flexible circuit assemblies.

## Acknowledgments

The CCAT project, FYST and Prime-Cam instrument have been supported by generous contributions from the Fred M. Young, Jr. Charitable Trust, Cornell University, and the Canada Foundation for Innovation and the Provinces of Ontario, Alberta, and British Columbia. The construction of EoR-Spec is supported by NSF grant AST-2009767. The construction of the 350 GHz instrument module for Prime-Cam is supported by NSF grant AST-2117631. The construction of the FYST telescope was supported by the Großgeräte-Programm of the German Science Foundation (Deutsche Forschungsgemeinschaft, DFG) under grant INST 216/733-1 FUGG, as well as funding from Universität zu Köln, Universität Bonn and the Max Planck Institut für Astrophysik, Garching.

S. Walker acknowledges support from the National Science Foundation under Award No. 2503181.

## References

[1] Z. B. Huber *et al.*, "CCAT: Prime-Cam optics overview and status update," *Proc. SPIE Int. Soc. Opt. Eng.*, vol. 13102, p. 1310222, 2024.

[2] F. Cortés, K. Cortés, R. Reeves, R. Bustos, and S. Radford, "Twenty years of precipitable water vapor measurements in the Chajnantor area," *Astronomy and Astrophysics*, vol. 640, p. A126, Aug. 2020.

[3] T. Nikola *et al.*, "CCAT-prime: the epoch reionization spectrometer for primce-cam on FYST," in *Millimeter, Submillimeter, and Far-Infrared Detectors and Instrumentation for Astronomy XI*, J. Zmuidzinas and J.-R. Gao, Eds., vol. 12190, International Society for Optics and Photonics. SPIE, 2022, p. 121900G. [Online]. Available: https://doi.org/10.1117/12.2629338

[4] C.-P. Collaboration, "Ccat-prime collaboration: Science goals and forecasts with prime-cam on the fred young submillimeter telescope," *The Astrophysical Journal Supplement Series*, vol. 264, no. 1, p. 7, dec 2022. [Online]. Available: https://dx.doi.org/10.3847/1538-4365/ac9838

[5] E. M. Vavagiakis *et al.*, "CCAT-prime: design of the Mod-Cam receiver and 280 GHz MKID instrument module," in *Millimeter, Submillimeter, and Far-Infrared Detectors and Instrumentation for Astronomy XI*, J. Zmuidzinas and J.-R. Gao, Eds., vol. 12190, International Society for Optics and Photonics. SPIE, 2022, p. 1219004. [Online]. Available: https://doi.org/10.1117/12.2630115

[6] C. J. Duell, E. M. Vavagiakis *et al.*, "Ccat-prime: Designs and status of the first light 280 ghz mkid array and mod-cam receiver," in *Millimeter, Submillimeter, and Far-Infrared Detectors and Instrumentation for Astronomy X*, J. Zmuidzinas and J.-R. Gao, Eds. SPIE, Dec. 2020, p. 58. [Online]. Available: http://dx.doi.org/10.1117/12.2562757

[7] A. I. Huber *et al.*, "CCAT-prime: optical and cryogenic design of the 850 GHz module for Prime-Cam," in *Millimeter, Submillimeter, and Far-Infrared Detectors and Instrumentation for Astronomy XI*, J. Zmuidzinas and J.-R. Gao, Eds., vol. 12190, International Society for Optics and Photonics. SPIE, 2022, p. 121901D. [Online]. Available: https://doi.org/10.1117/12.2630370

[8] M. Neric *et al.*, "Characterization of cryogenic flexible transmission lines designed for the gusto if harness," in *Proceedings of the 31st Symposium on Space Terahertz Technology, ISSTT 2020*, ser. Proceedings of the 31st Symposium on Space Terahertz Technology, ISSTT 2020. International Symposium on Space Terahertz Technology, 2020, pp. 50–53, publisher Copyright: © 2020 Proceedings of the 31st Symposium on Space Terahertz Technology, ISSTT 2020. All rights reserved.; 2020 31st IEEE International Symposium on Space Terahertz Technology, ISSTT 2020 ; Conference date: 08-03-2020 Through 11-03-2020.

[9] N. Simon, E. Drexler, and R. Reed, "Properties of copper and copper alloys at cryogenic temperatures. final report," National Inst. of Standards and Technology (MSEL), Boulder, CO (United States). Materials Reliability Div., Tech. Rep., 01 1992. [Online]. Available: https://www.osti.gov/biblio/5340308

[10] D. L. Rule, D. R. Smith, and L. L. Sparks, "Thermal Conductivity of a Polymide Film Between 4.2 and 300K, with and without Alumina Particles as Filler," 8 1990.

[11] H. Terry *et al.*, "The CCAT-Prime Submillimeter Observatory," in *Bulletin of the American Astronomical Society*, vol. 51, Sep. 2019, p. 213.